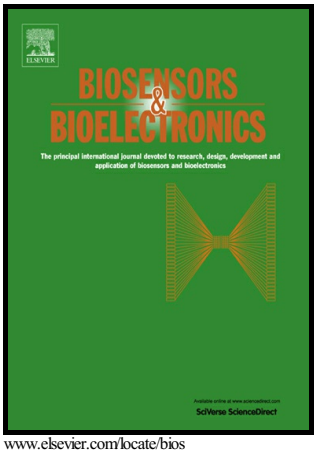

www.elsevier.com/locate/bios

Non-invasive, in vitro analysis of islet insulin production enabled by an optical porous silicon biosensor

Rinku Chhasatia, Martin J. Sweetman, Frances J. Harding, Michaela Waibel, Tom Kay, Helen Thomas, Thomas Loudovaris, Nicolas H. Voelcker

PII: S0956-5663(17)30003-9
DOI: http://dx.doi.org/10.1016/j.bios.2017.01.004
Reference: BIOS9469

To appear in: *Biosensors and Bioelectronic*

Received date: 29 September 2016
Revised date: 27 December 2016
Accepted date: 3 January 2017

Cite this article as: Rinku Chhasatia, Martin J. Sweetman, Frances J. Harding Michaela Waibel, Tom Kay, Helen Thomas, Thomas Loudovaris and Nicolas H. Voelcker, Non-invasive, in vitro analysis of islet insulin production enabled by ar optical porous silicon biosensor, *Biosensors and Bioelectronic* http://dx.doi.org/10.1016/j.bios.2017.01.004

Non-invasive, *in vitro* analysis of islet insulin production enabled by an optical porous silicon biosensor

Rinku Chhasatia[a], Martin J. Sweetman[b], Frances J. Harding[a], Michaela Waibel[c], Tom Kay[c], Helen Thomas[c], Thomas Loudovaris[c], Nicolas H. Voelcker[a*]

[a]ARC Centre of Excellence in Convergent Bio-Nano Science and Technology, Future Industries Institute, University of South Australia, Mawson Lakes, South Australia 5095, Australia

[b]Experimental Therapeutics Laboratory, Hanson Institute and Samson Institute, School of Pharmacy and Medical Sciences, University of South Australia, Adelaide, SA 5000, Australia

[c]St. Vincent's Institute of Medical Research, Victoria 3065, Australia

E-mail nico.voelcker@unisa.edu.au (N.H. Voelcker)

[*]Correspondence to: GPO Box 2471, Adelaide, South Australia 5001, Australia. , Tel: +61 8 8302 5508

Abstract

A label-free porous silicon (pSi) based, optical biosensor, using both an antibody and aptamer bioreceptor motif has been developed for the detection of insulin. Two parallel biosensors were designed and optimised independently, based on each bioreceptor. Both bioreceptors were covalently attached to a thermally hydrosilylated pSi surface though amide coupling, with unreacted surface area rendered stable and low fouling by incorporation of PEG moieties. The insulin detection ability of each biosensor was determined using interferometric reflectance spectroscopy, using a range of different media both with and without serum. Sensing performance was compared in terms of response value, response time

and limit of detection (LOD) for each platform. In order to demonstrate the capability of the best performing biosensor to detect insulin from real samples, an *in vitro* investigation with the aptamer-modified surface was performed. This biosensor was exposed to buffer conditioned by glucose-stimulated human islets, with the result showing a positive response and a high degree of selectivity towards insulin capture. The obtained results correlated well with the ELISA used in the clinic for assaying glucose-stimulated insulin release from donor islets. We anticipate that this type of sensor can be applied as a rapid point-of-use biosensor to assess the quality of donor islets in terms of their insulin production efficiency, prior to transplantation.

Keywords*:* Porous silicon, optical biosensor, insulin, interferometric reflectance spectroscopy, aptamer, islet

1.Introduction

Type 1 diabetes is an auto-immune disease in which the beta cells of islets of Langerhans, responsible for production of insulin, are attacked and destroyed by the body's own immune system. The destruction of beta cells in the pancreas results in the inability to produce sufficient insulin, and as a result high blood glucose levels that can lead to severe long-term organ damage (Alberti and Zimmet 1998; Atkinson et al. ; Inzucchi and Sherwin 2011). There is currently no prevention or cure for type 1 diabetes, and the early onset of this condition exposes patients to more severe health repercussions and thus requires lifelong careful management of blood glucose levels by multiple daily insulin injections (Chiang et al. 2014). Even with advances in management strategies, recent research still highlights a significant loss of life expectancy, approximately 11 years for men and 13 years for women

with type 1 diabetes (Livingstone et al. 2015). These factors emphasize the need for novel diagnosis and treatment methods.

The most promising alternative treatment for type 1 diabetes is in form of islets transplantation. This treatment is indicated for patients with hypoglycemic unawareness, who have significantly high mortality rate (Cryer 2011; Feltbower et al. 2008; Nathan 2014; Skrivarhaug et al. 2006). In this process, islets are isolated from a donor and, in the most common protocols, infused into the portal vein of a type 1 diabetic patient through a catheter, where they lodge in the liver (Paty 2005; Piper et al. 2004).. Islet transplantation reduces or eliminates the need for insulin injections and reduces the occurrence of severe hypoglycemic episodes (Rickels et al. 2005; The National Institute of Diabetes and Digestive and Kidney Diseases US). Recently, significant progress has been made in the field of islets transplantation; however, many challenges remain that prevent its widespread application, such as donor shortage, transplant failure and the need for lifelong immuno-suppressive therapy (Bottino and Trucco 2015; Leitão et al. 2008; Montane 2015; Rother and Harlan 2004; The National Institute of Diabetes and Digestive and Kidney Diseases US). One of the key challenges of islet transplantation is the assessment of donor islet function by insulin production efficiency before transplantation, since loss of islet function *ex vivo* is a key determinant of transplant failure (Kin et al. 2008; Rother and Harlan ; Trabucchi et al. 2014; Van Der Windt et al. 2007). The average pancreatic insulin content is ~10 µM (Cha et al. 2011). When it comes to *in vitro* analysis of islets for insulin secretion, this values depends various factors such as number and size of islets, amount and duration for which glucose stimulation is performed. Currently available methods to determine insulin output include enzyme linked immunosorbent assay (ELISA), radio immunoassay (RIA), chromatography and mass spectroscopy (Farino et al. 2016; Kekow et al. 1988; Luo et al. 2013; Ohkubo

1994). These techniques are typically laborious, time consuming and expensive, while also requiring sophisticated laboratory equipment and trained personnel. In addition, some of these methods require the labelling of insulin, which can affect its intrinsic properties and hence can affect the assay result (Daniels and Pourmand 2007; Huh et al. 2011; Sang et al. 2013). Importantly, none of these methods has the capacity for direct, point of use monitoring of glucose-stimulated insulin secretion, which is essential to assess the islets for their insulin secretion efficiency before transplantation (Cha et al. 2011). The ideal system to determine insulin production from donor islets would be an *in situ*, label-free, non-invasive sensor that could report the insulin level. The development of such a biosensor has remained a challenge, but would likely provide significant benefit to the islet transplantation treatment process.

The analytical efficiency of any biosensor is highly dependent on the bioreceptor conjugated to it, which should impart a high degree of specificity to the sensor (Vo-Dinh and Cullum 2000). To date, antibodies are the most extensively employed bioreceptors, not only for fabrication of biosensors but also in standard immunoassay analysis (Schumacher and Seitz 2016; Steward and Lew 1985; Strehlitz et al. 2008). This is because of their unique ability to selectively bind to their target molecule (Mariuzza et al. 1987; Vo-Dinh and Cullum 2000). Additionally, the commercial availability of antibodies has contributed to their widespread application as bioreceptors. Although antibodies possess several unique advantages, there are certain drawbacks that would justify an alternative option, such as high cost, large size, instability and they are usually produced in animals, which raises ethical concerns and can also result in batch-to-batch variation (Mairal et al. 2008; Song et al. 2008; Zhou et al. 2014). Aptamers are the most promising alternative to antibodies. An aptamer is a single stranded DNA or RNA that when folded into a specific conformation is known to mimic the function

of an antibody. Despite numerous advantages of aptamer over antibodies, the complete replacement of antibody receptors with aptamers is not likely due to the limited number of examples that demonstrate the use of aptamers as an effective bioreceptor. The beauty of aptamers is that they possess several distinct advantages over antibodies such as cost effectiveness, smaller size, high stability. Importantly, they can be easily synthesised in a laboratory by the SELEX (systematic evolution of ligand by exponential enrichment) process (Song et al. 2008; Zhou et al. 2014). On top of these advantages, aptamers offer at least equivalent or in some cases higher selectivity and affinity than antibodies (Mairal et al. 2008; Tombelli et al. 2007).

Recently, porous silicon (pSi) has received considerable interest as a material to construct low cost, sensitive and biocompatible optical biosensors (Alhmoud et al. 2015; Krismastuti et al. 2014a; Krismastuti et al. 2013; McInnes et al. 2015; Reta et al. 2016; Tong et al. 2016). This is due to its captivating features such as availability at relatively low cost, simple fabrication process and inherent optical properties, which allows the design of high performance, simple, compact biosensors (De la Mora et al. 2013; Dhanekar and Jain 2013). Relevant biosensing properties of pSi can be optimised to suit specific applications, including pore size, pore depth and porosity, which is achieved simply by controlling the etching parameters (De Stefano et al. 2015; Jane et al. 2009). The high surface area to volume ratio of pSi (up to 800 m^2/g) facilitates the attachment of a large number of bio-receptors and hence enhances the sensitivity of the fabricated biosensor (Basu and Kanungo 2011; Steiner and Lang 1995). Further to these advantageous properties, pSi is biocompatible and biodegradable, making it an ideal candidate for use as a sensing scaffold for various biomedical applications (Coffer et al. 2005; Low et al. 2009; Shabir 2014). Hence, the combination of the distinctive properties of pSi, coupled with a suitable transduction

mechanism, provides a means to fabricate highly selective, sensitive and label-free, non-invasive biosensors.

Amongst the various pSi biosensor devices currently available, optical biosensors using interferometric reflectance spectroscopy (IRS) offer distinct advantages (Monošík et al. 2012; Perumal and Hashim 2014; Vo-Dinh 2014) . This technique enables label-free, remote sensing with an extremely simple set up (Dancil et al. 1999; Lin et al. 1997; Shang et al. 2010), providing an ideal method for various cell and tissue culture analysis. In IRS, 90° incident white light is reflected from the two interfaces (air-pSi and pSi-bulk Si) of the porous material to produce a Fabry-Perot interference fringe pattern, dependent on the optical thickness and refractive index (n) of the porous material, (Janshoff et al. 1998; Lérondel 2015; Pacholski et al. 2005). The fringe pattern is described by equation 1;

Eq. 1 $$m\lambda = 2nL$$

λ = maximum wavelength of consecutive fringe order of magnitude *m*, *L* is the thickness of the porous layer and '*2nL*' is called the effective optical thickness (EOT). The EOT can be determined directly by applying a Fast Fourier Transformation (FFT) to the observed interference fringe pattern and is often the parameter used to measure sensor response. When an analyte is captured within the porous matrix by a tethered bioreceptor moiety, a resultant red shift of the fringe pattern is observed. The induced red shift is due to the replacement of water (n = 1.33) within the pores with protein, which has a higher refractive index (n ≈ 1.45) (Jane et al. 2009; Lin et al. 1997). This results in an increase of the net refractive index within the porous matrix and hence an increase in the EOT value (observed as a red shift of the fringe pattern) (Dancil et al. 1999; Jane et al. 2009; Pacholski et al. 2005). Thus, IRS enables the detection of analytes simply by monitoring changes to the EOT over time.

There are many examples of pSi-based optical biosensors in the literature, applied to the detection of various biomolecules such as proteins, enzymes, DNA and even whole cells (Choi et al. 2012; Dancil et al. 1999; Holthausen et al. 2012; Krismastuti et al. 2013; Lin et al. 1997; Merkl et al. 2012; Pacholski et al. 2005). However, to the best of our knowledge, this platform has not been applied for the detection of insulin and neither to the direct detection of hormones produced by primary human tissues. To date, label-free insulin biosensors have relied on electrochemical techniques, measuring from buffer (Qu et al. 2006; Rafiee and Fakhari 2013; Wang and Musameh 2004; Wang et al. 2007; Yu et al. 2016) or in some cases from serum (Luo et al. 2013; Singh and Krishnan 2015; Yagati et al. 2016), but not from islets suspensions. Tae-Gon Cha and colleagues approached a label-free detection of insulin secreted from islets. However, this was achieved by using fluorescent single wall carbon nanotubes (Cha et al. 2011).

Herein, we aimed to design a label-free pSi based optical biosensor for the detection of insulin secreted by human pancreatic islets. For this, single layer pSi was used as the biosensing platform and functionalised by applying the commonly used hydrosilylation method. This generic surface chemistry allows two different bio-receptor interfaces to be prepared in parallel. The first interface involved an antibody-modified surface (Ab-modified) and secondly an aptamer-modified surface (Ap-modified). Following conjugation of the bioreceptors, unreacted surface sites were passivated with a poly(ethylene glycol) (PEG) compound. PEG passivation has been shown to prevent non-specific binding (Raftery et al. 2016; Sharma et al. 2004; Yu et al. 2011) to the prepared interfaces during the biosensing process. The biosensing performance and calibration of both interfaces was evaluated in Krebs Ringer buffer; a commonly employed buffer used for the glucose-stimulated insulin secretion (GSIS) assay in the clinic (Grant et al. 1980; Pi et al. 2007; Qureshi et al. 2015).

Finally, we demonstrated insulin detection using the Ap-modified biosensor from a real sample, i.e. insulin secreted by human islets on stimulation with glucose. One of the most significant aspects of insulin detection in the real sample is that the sample required no pre-treatment and could be applied directly to the pSi biosensor interface.

2. Materials and Methods

2.1 Materials and reagents

Silicon wafers (boron doped $p^{++} \leq 0.002$ Ω cm resistivity) were purchased from Siegert (Germany). Hydrofluoric Acid (HF 48 %) was purchased from Scharlau (Australia). Ethanol and acetone were purchased from Chem-Supply (Australia). Sodium hydroxide was purchased from Merck (Australia). Rabbit polyclonal insulin antibody was obtained from Santa Cruz Biotechnology (USA). The newly developed 30-mer insulin binding aptamer (5'-GGT GGT GGG GGG GGT TGG TAG GGT GTC TTC-3') (Yoshida et al. 2009); 3' modified with -NH_2, was synthesised by Gene Works (Australia). Rat/Mouse insulin ELISA kits were obtained from Millipore, USA. All other chemical were purchased from Sigma-Aldrich (Australia) unless otherwise mentioned.

2.2 Fabrication of pSi single layer structures

Two pSi single layer (pSiSL) structures were fabricated with different pore sizes; larger pore size (pSiSL-1) and smaller pore size (pSiSL-2). Etching was carried out by applying an electrochemical anodisation process in a 1:1 HF:ethanol (48 % HF:absolute ethanol) solution. Etching was performed in a custom-built Teflon cell, connected to a source meter (2425 Keithley, USA). An Al sheet placed at the back side of the Si wafer acted as an anode while platinum mesh acted as cathode (Jamois et al. 2011; Mora et al. 2013; Wang et al. 2012) .

pSiSL-1 and pSiSL-2 were fabricated by applying a current density of 95 mA/cm^2 for 30 s and 35 mA/cm^2 for 100 s, respectively. Etching was performed in a two-step process with the previously mentioned etching parameters used for both the steps in the fabrication of pSiSL-1 and pSiSL-2 samples. In the first step, a parasitic pSi layer was formed which was dissolved with 1 M NaOH after anodisation (Sciacca et al. 2011), followed by three times washing with MilliQ water and ethanol, before drying with compressed air. The second etching step was performed by applying the same etching parameters as for step one. The second etching step produced the working pSi film, pSiSL-1 or pSiSL-2. The morphology of the prepared pSiSLs were analysed by scanning electron microscopy (SEM) to determine pore size and thickness of the porous layer.

2.3 pSiSL functionalisation

(A) Thermal hydrosilylation

Freshly etched pSiSLs were subjected to a thermal hydrosilylation reaction with neat undecylenic acid (UA) at 150 °C for 24 h under a constant flow of N_2(g). The modified samples (denoted pSiSL-1-UA and pSiSL-2-UA), were washed with copious amount of ethanol, dried and stored in a desiccator until further surface reaction.

(B) 1-ethyl-3-(3-dimethylaminopropyl) carbodiimide (EDC)/ N-hydroxysuccinimide ester (NHS) activation

pSiSL-1-UA and pSiSL-2-UA were allowed to react with EDC/NHS to form pSiSL-1-NHS and pSiSL-2-NHS, respectively. For this reaction, the pSiSLs were reacted in a 5 ml solution of 1:1 mixture of 10 mM EDC and 10 mM NHS in 1 x phosphate buffer saline (PBS) for 1 h

at room temperature. The surfaces were then rinsed three times with MilliQ water and 1 x PBS. NHS ester functionalised surfaces were used immediately for conjugation of the bioreceptors.

(C) Attachment of bioreceptor

(i) Attachment of antibody

pSiSL-1-NHS was reacted with 30 µg/ml insulin antibody in 1 x PBS with agitation for 3 h at room temperature, followed by overnight incubation at 4 °C (Holthausen et al. 2012; Krismastuti et al. 2014b; Krismastuti et al. 2016; Reta et al. 2016). The surface was then washed with MilliQ water and 1 x PBS to produce pSiSL-1-Ab.

(ii) Attachment of aptamer

pSiSL-2-NHS was reacted with insulin-binding aptamer, 50 µM in TKN (50 mM Tris–HCl, 10 mM KCl, 100 mM NaCl, pH 8.0) buffer. The reaction time and temperature was the same as in the case of antibody immobilisation. Importantly, before being immobilised, the aptamer solution was heated up to 95 °C for 5 min and then allowed to cool down for at least 20 min at room temperature prior to surface immobilisation. Aptamer conjugation produced surface pSiSL-2-Ap.

(D) Blocking

Finally, blocking of residual active NHS sites on both surfaces (pSiSL-1-Ab and pSiSL-2-Ap) was carried out by reaction with 1 mg/ml bis PEG-amine (BPA) (3000 Mw) for 1 h in 1 x PBS and TKN buffer for pSiSL-1-Ab and pSiSL-2-Ap, respectively. This was followed by washing with MilliQ water to complete the fabrication of Ab-modified and Ap-modified

interfaces, respectively. Ab-modified surfaces were stored in PBS and Ap-modified in TKN buffer at 4 °C prior to use in sensing experiments.

2.4 Characterisation methods

2.4.1 Scanning electron microscopy (SEM)

SEM images were obtained on a Quanta 450 field emission gun environmental scanning electron microscope, equipped with a solid state detector and operated at voltage of 30 kV. The images were analysed using Image J software (1.48v).

2.4.2 Fourier transform infrared (FTIR) spectroscopy

Surface characterisation of the prepared bio-recognition interfaces at each functionalisation step was performed using an FTIR microscope (Hyperion 1000, Bruker, Germany). The microscope is equipped with a Vertex 70 IR source coupled to a liquid nitrogen cooled Mercury-Cadmium-Telluride (MCT) detector. IR spectra were collected in reflection mode. All spectra were recorded between the range of 400 cm^{-1} to 4000 cm^{-1} with a 4 cm^{-1} resolution and averaging 64 scans. Flat unetched silicon wafer was used as a background for the analysis. All spectra were collected and processed using Opus 7.2 software.

2.4.3 Flow cell and interferometric reflectance spectroscopy (IRS)

Optical sensing experiments were performed using an interferometric reflectance spectroscope, operated at room temperature. A pSi sample was clamped into a custom-made

plexiglass flow cell which was then connected to a peristaltic pump to allow solution to flow through it at flow rate of 1.5 ml/min. White light (halogen light source HL-2000, Ocean Optics) was focused onto the pSi surface through the plexiglass flow cell at 90^{o} incident angle using a bifurcated fibre optic probe. The reflectance spectrum of the pSi was measured using a charge couple device (CCD) spectrometer (USB 2000, Ocean Optics) connected to the output end of bifurcated optic cable. Data was recorded using Laboratory View software (8.2.1 version), analysed using Wavemetric Inc. Igor program and plotted with Origin (9.1.0).

2.5 Insulin detection in buffer

Detection of insulin supplemented into Krebs buffer was performed using both the Ab-modified and Ap-modified pSi interfaces at concentrations of 5 µg/ml, 10 µg/ml, 20 µg/ml, 30 µg/ml, 40 µg/ml and 50 µg/ml. The reflectance spectra were collected at per min intervals using IRS. For the first 20 min, Krebs buffer (no insulin) was introduced to the biosensor surface to establish a baseline, followed by insulin solution in Krebs buffer (80 min for Ab-modified, 60 min for Ap-modified). Signal change specificity to insulin was achieved by reintroduction of Krebs buffer (no insulin) for 20 min as the third stage of detection. The control experiments were performed in a same way, using sensors in which a non-specific antibody and non-specific control DNA was conjugated to the Ab- and Ap-modified pSi interfaces respectively. The sensing capability of the pSi interfaces was also tested in different media including PBS, cell culture medium (CLM) (without serum) and CLM (with serum) (data for these sensorgrams is provided in the Supporting Information).

2.6 Detection of insulin from real sample

Human islets of Langerhans allocated for research use were provided by the St. Vincent's Institute of Medical Research, Victoria, Australia. Approval for research use of human islets

was obtained from the Royal Adelaide Hospital and University of South Australia research ethics committees (protocol number 0000033541). Human islets were cultured in CMRL 1066 medium supplemented with 15 % fetal calf serum, 2 mM GlutaMax, 10 mM HEPES at 37 °C and 5 % CO_2. The Ap-modified surface was applied for the detection of insulin from a real sample of glucose-stimulated human islets. 40,000 IEQ (islet equivalents) were stimulated with a 10 ml solution of 20 mM glucose in Krebs buffer for 2 h to induce insulin secretion. Following stimulation, the cells were pelleted by centrifugation and the supernatant was collected and used for sensing experiments on the Ap-modified surface. For this, Krebs buffer (with 20 mM glucose) was firstly flowed over the pSi surface for 20 min, followed by the collected supernatant for 100 min, and then finally washing with Krebs buffer (20 mM glucose) for 20 min. The control experiment was performed in same manner but with a pSi surface modified with negative control DNA oligonucleotide instead of the aptamer. Validation of the insulin content of islet-conditioned Krebs buffer samples was performed via insulin ELISA (EMD Millipore), according to the manufacturer's instructions. Islet conditioned Krebs buffer samples were diluted 1/1000 before analysis. A standard curve constructed in the range 1-100 ng/ml human insulin was fitted to a four parameter sigmoidal function (Prism, Graphpad) and the content of the islet-conditioned samples interpolated from this standard curve. Measurement of samples and standards was performed in triplicate.

3. Result and Discussion

3.1 Fabrication and characterisation of pSiSLs

In this study, two pSiSL structures were fabricated using a two-step electrochemical anodisation process. The resulting surface and internal pore structure was characterised by SEM. pSiSL-1 and pSISL-2 were fabricated by applying a current density of 95 mA/cm^2 for 30 s and 35 mA/cm^2 for 100 s, respectively. Figure S1 displays the top view (a-b) and cross section (c-d) SEM images for pSiSL-1 and pSiSL-2, respectively. The resulting pore size of pSiSL-1 was ~ 72 nm, which was large enough to allow ingress of the IgG antibody (150 kDa). This surface was subsequently used for the fabrication of Ab-modified biosensor. pSiSL-2 resulted in a pore size of ~ 27 nm, and was used for the fabrication of Ap-modified surface since the aptamer (9.7 kDa) is much smaller than the antibody. The thickness of both pSiSLs was approximately 1.2 µm.

3.2 pSiSL functionalisation

Surface modification of the freshly etched pSiSLs was essential in order to fabricate highly selective and sensitive biosensors. Figure 1 shows a schematic diagram for the pSi surface functionalisation process used to generate interfaces for the detection of insulin. The process begins with freshly etched pSiSL subjected to (a) a thermal hydrosilylation reaction with undecylenic acid, followed by reaction with (b) EDC/NHS and then (c) immobilisation of antibody or aptamer and, finally (d) quenching of active NHS ester with BPA.

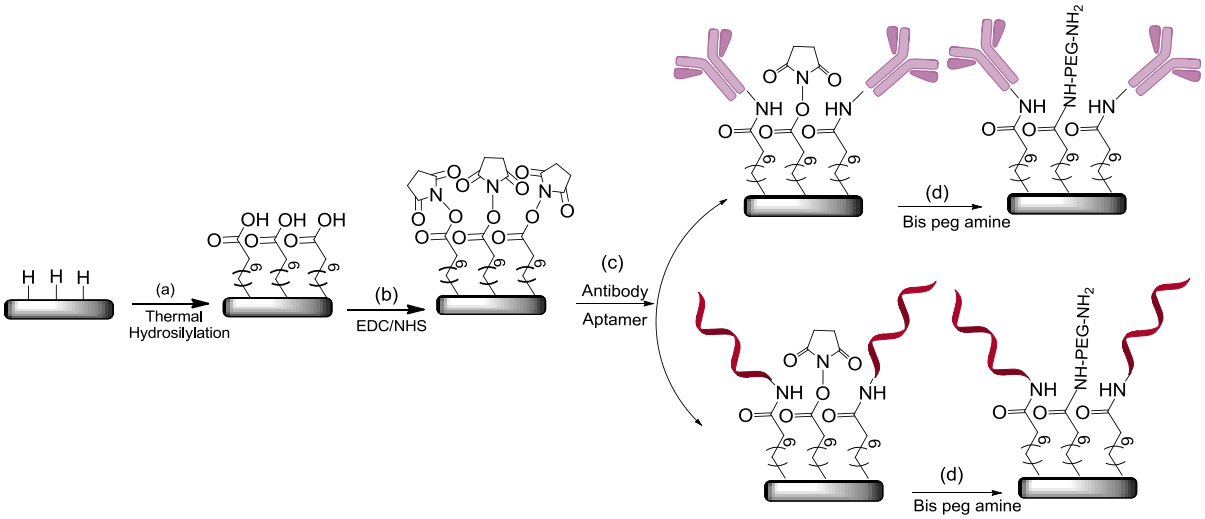

Figure 1: Schematic of surface modification steps involved during fabrication of pSi biosensors for the detection of insulin: (a) thermal hydrosilylation of freshly etched pSi, (b) EDC/NHS activation, (c) immobilisation of the respective bio-receptor and (d) quenching with BPA.

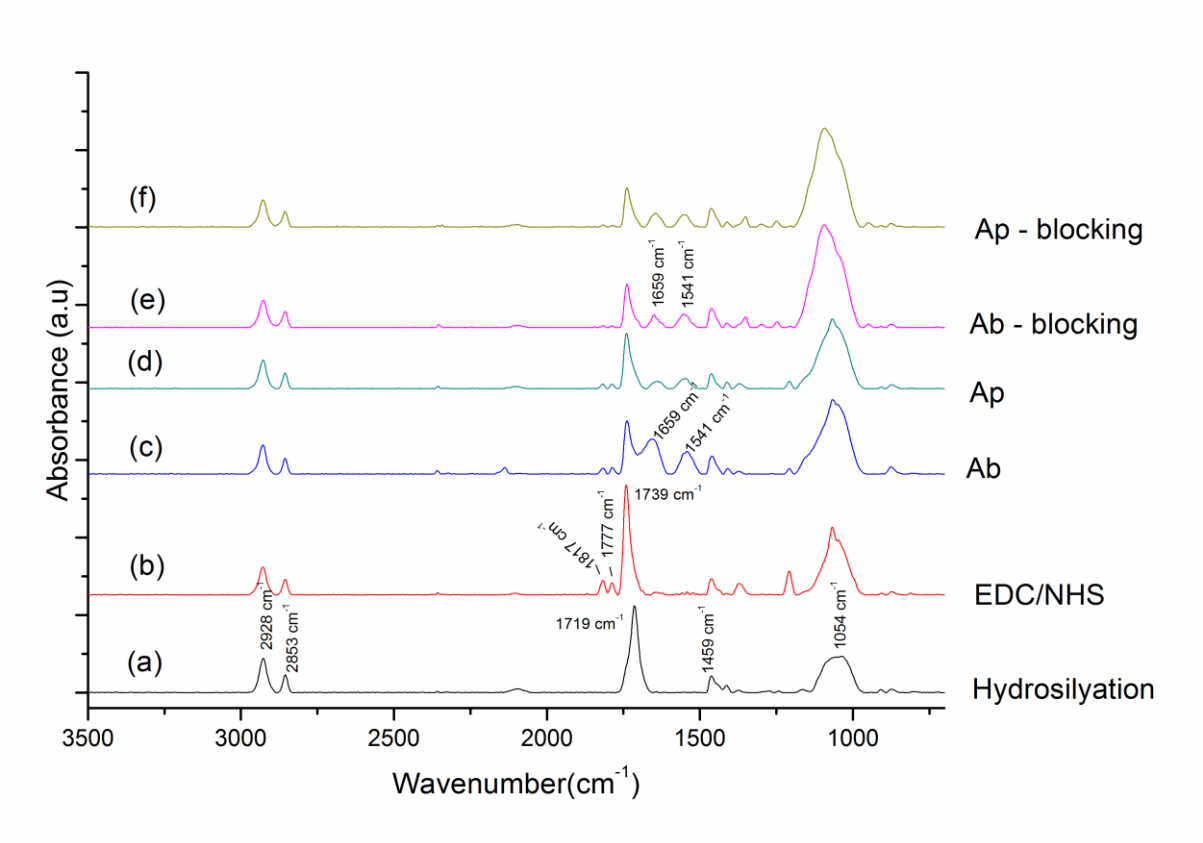

Figure 2: FTIR spectra collected in reflectance mode for each step of pSi surface functionalisation. (a) Thermal hydrosilylation, (b) EDC/NHS activation, (c) reaction with Ab, (d) reaction with Ap, (e) blocking of NHS ester on Ab-immobilised surface with BPA and (f) blocking of NHS ester on Ap-immobilised pSi with BPA.

Characterisation at each step of the surface modification procedure was performed by FTIR spectroscopy, in reflectance mode (Figure 2). All spectra were collected using the larger pore size pSiSL-1 surface geometry (~ 72 nm) in order to avoid an interference effect observed when analysing the small pore size pSi (Voelcker et al. 2008). The displayed spectra have also been baseline corrected using Opus software.

Firstly, a thermal hydrosilylation reaction with neat undecylenic acid was performed on freshly etched pSiSL (spectrum a). The IR spectrum for this surface showed peaks at 2928 cm^{-1}, 2853 cm^{-1}, and 1454 cm^{-1}, corresponding to aliphatic chain C-H stretching vibrations and deformation vibration of methylene group, respectively (Krismastuti et al. 2013; Sweetman et al. 2012; Sweetman et al. 2011b). The additional sharp peak at 1719 cm^{-1} is attributed to the -C=O stretching vibration from the terminal carboxylic acid group of undecylenic acid (Krismastuti et al. 2013; Sweetman et al. 2012; Sweetman et al. 2011b). The presence of these bands clearly confirms success of the thermal hydrosilylation reaction and indicated the formation of a dense alkyl monolayer onto the pSiSL surface. Formation of such an alkyl monolayer is known to protect the pSi surface from hydrolytic attack and hence should impart stability to the porous structure (Krismastuti et al. 2013; Sweetman et al. 2011a). However, the observation of a blue shift of the baseline during the sensing experiments (Figure 4, section I), indicates slight degradation of the modified surfaces. This degradation is attributed to the presence of residual Si-O_x species, confirmed by the presence

of a peak at 1054 cm^{-1} and indicates some oxidation of the Si-H surface (Krismastuti et al. 2013; Szili et al. 2011). The oxidation likely occurred during the hydrosilylation reaction and handling of the pSi surface in air (Flavel et al. 2011; Sweetman et al. 2011a).

The –COOH terminated pSiSL was then activated with NHS in the presence of EDC, to make the functionalised surface amine reactive (spectrum b). The peaks at 1739 cm^{-1} and 1777 cm^{-1} can be assigned to the antisymmetric stretching and symmetric stretching vibrations from the carbonyl groups of the incorporated succinimidyl ring, respectively (Holthausen et al. 2012; Reta et al. 2016). In addition, the peak at ~ 1817 cm^{-1} belongs to symmetric stretching vibration of the succinimidyl carbonyl ester (Touahir et al. 2010). The appearance of peaks for the NHS ester are indicative of successful EDC/NHS reaction.

Following the reaction with NHS ester, pSiSL surfaces were allowed to react with bioreceptors; Ab (spectrum c) and Ap (spectrum d). In both spectra, the peaks exhibited at 1659 cm^{-1} and 1541 cm^{-1}, are attributed to amide (I) and amide (II) bonds, respectively (Flavel et al. 2011; Krismastuti et al. 2013; Reta et al. 2016). These peaks strongly indicate that both bioreceptors have been covalently attached to the pSi surfaces through amide bonds. However, the presence of the triplet peaks of the NHS ester following bioreceptor conjugation indicates that some of this species remains unreacted. This is expected, as the large size of the biomolecules will sterically hinder complete conjugation to all active NHS ester sites within the porous matrix (Flavel et al. 2011; Krismastuti et al. 2013).

In the last step, quenching of active NHS ester sites was performed by reaction with BPA of 3,000 Da. A terminal amine group of the BPA reacted with the residual NHS ester via formation of a covalent amide bond and resulted in the disappearance of the peaks at 1817

cm^{-1} and 1777 cm^{-1} (spectra e and f). This confirms the successful quenching of active NHS esters on the bioreceptor-immobilised pSi surface (Flavel et al. 2011; Reta et al. 2016). Along with quenching the remaining reactive NHS esters, inclusion of the PEG moiety to the modified interfaces can also effectively control non-specific binding and thus contribute to the selectivity and sensitivity of the biosensor (Raftery et al. 2016; Sharma et al. 2004; Sweetman et al. 2011b; Yu et al. 2011).

3.3 Detection of insulin

Both of the prepared interfaces (i.e. Ab-modified and Ap-modified surfaces) were investigated as an optical biosensing platform for the detection of insulin in Krebs buffer. Detection of insulin in other media, including PBS, CLM and CLM with serum, was also investigated and is presented in the Supporting Information.

3.3.1 Sensing on Ab-modified surface

Figure 3 represents a typical sensorgram for the detection of insulin by the Ab-modified pSi surface. The Ab-modified surface was exposed to Krebs buffer solution with no insulin for 20 min in order to establish a baseline, before an insulin containing (50 µg/ml) Krebs buffer solution was introduced for 80 min, followed by a final wash with Krebs buffer for 40 min.

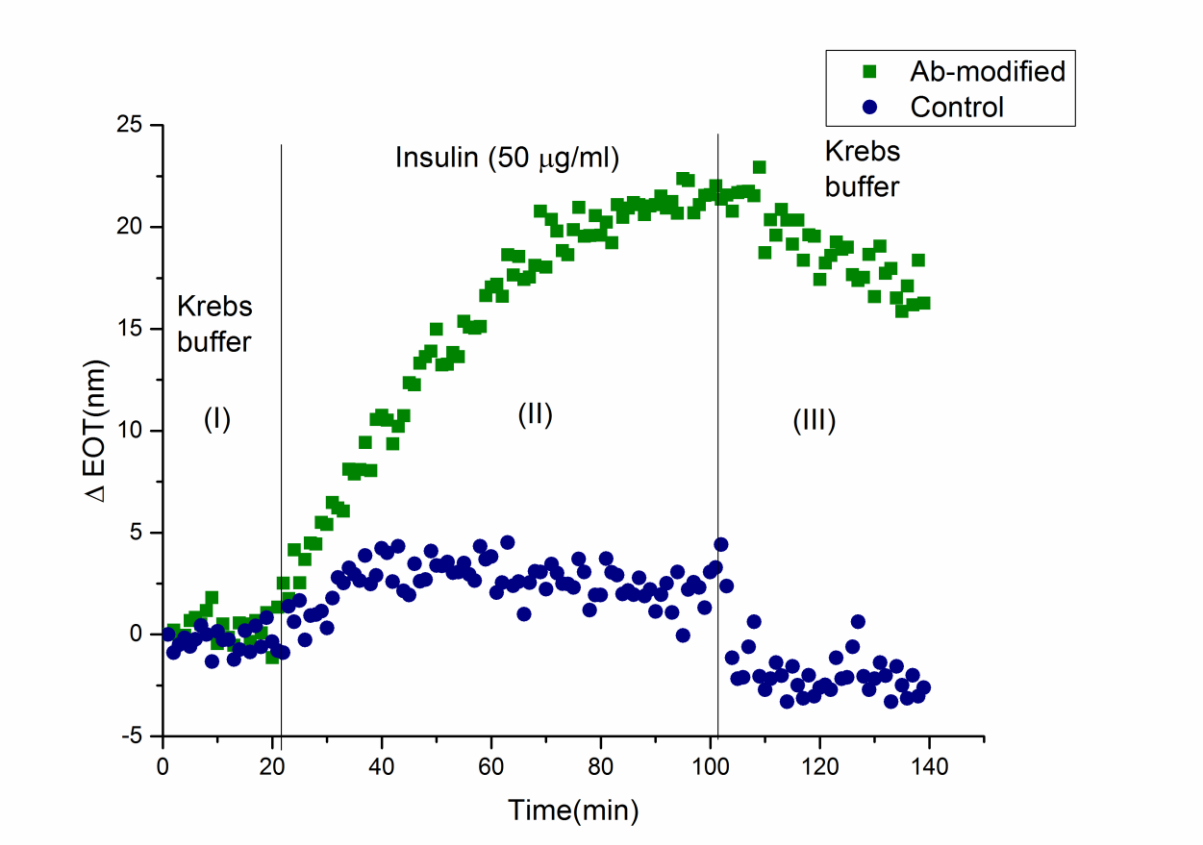

Figure 3: Sensorgrams of response to insulin (50 µg/ml) in Krebs buffer on Ab-modified pSi surface and control (non-specific Ab) pSi surface.

As shown in Figure 3, addition of Krebs buffer from 0 min to 20 min (section I) enables a baseline to be established where there are no significant changes in the ΔEOT value. When the insulin (50 µg/ml) solution was allowed to flow through the cell (section II) a significant increase in the ΔEOT was observed. During the first 60 min of insulin exposure, there was a steady increase in the ΔEOT value, amounting to a change of approximately 21 nm. This red shift is attributed to binding of insulin to the insulin-specific antibody present within the pores on the Ab-modified surface. This capture event causes an increase in the net refractive index of the porous layer and hence resulted in the increase of EOT. Between 82 – 103 min, no further increase in ΔEOT was observed. This plateau of the sensor response indicates saturation of the binding sites on the Ab-modified pSi surface or steric hindrance from bound

species preventing the ingress of more insulin into the pores. Finally, the Krebs buffer washing step (section III), resulted in a small blue shift (~ 5 nm), due to removal of unbounded or loosely bounded insulin to the surface. The control surface (blue graph) showed a slight red shift (~ 5 nm) on addition of insulin (section II) that is attributed to the combined effect of a small refractive index change in the bulk solution and a small amount of non-specific protein adsorption. However, the surface returned to baseline levels following the washing steps. Thus, overall no significant changes to ΔEOT values were observed on the control surface. This confirms that the observed red shift on the Ab-modified pSi surface was due to the selective binding of insulin into the pores. An overall red shift of ~ 16 nm, with respect to initial base line, was observed for insulin sensing on the Ab-modified pSi surface, with a maximum ΔEOT response reached in ~ 60 min.

3.3.2 Sensing on Ap-modified surface

Following the successful detection of insulin using the Ab-modified pSi surface, the same insulin detection procedure was applied to the Ap-modified surface, with the resulting sensorgrams for detection on Ap-modified and control surfaces displayed in Figure 4.

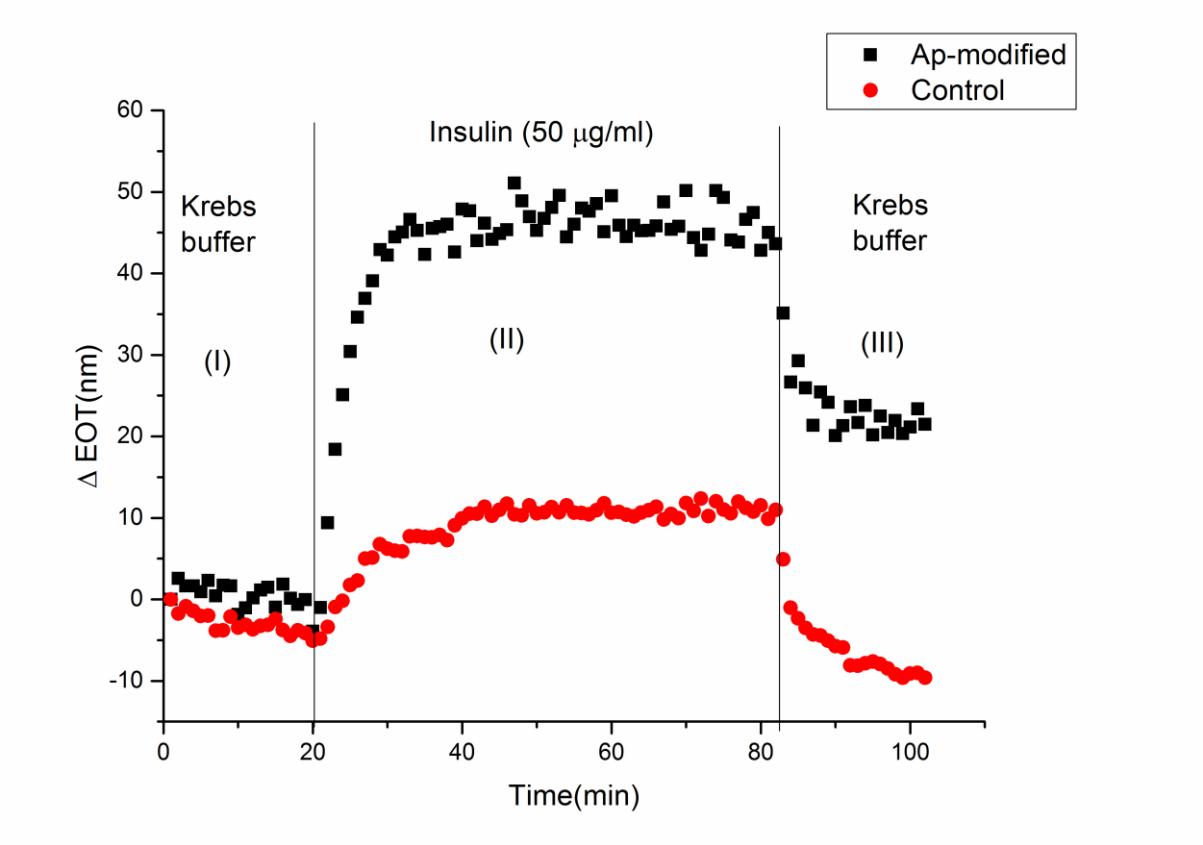

Figure 4: Sensorgrams of response to insulin (50 μg/ml) in Krebs buffer on Ap-modified pSi surface and control (non-specific DNA) pSi surface.

Insulin detection was performed under the same conditions as for the Ab-modified pSi surface, with Krebs buffer for first 20 min, followed by insulin (50 μg/ml) solution for 60 min and finally rinsing with Krebs buffer for 20 min. As expected, during the flow of Krebs buffer for first 20 min (section I), no change to ΔEOT was observed. Interestingly, on introduction of the insulin solution through the cell, the ΔEOT value increased dramatically (section II) and reached a maximum ΔEOT response (of ~ 40 nm), in just 12 min. Further incubation in the insulin solution (34 min to 82 min) did not result in any further changes to the ΔEOT value, which confirms saturation of the binding sites. The faster response time of the Ap-modified surface is attributed to the unique conformation change of the aptamer during interaction with the insulin, which allows rapid binding (Lei et al. 2015; Verdian-

Doghaei et al. 2015; Yoshida et al. 2009). Washing with Krebs buffer (section III), resulted in a blue shift of ~ 20 nm, due to removal of unbounded insulin. Thus, the Ap-modified pSi surface displayed an overall red shift of ~ 19 nm and maximum response was achieved in a time of 12 min, for insulin at 50 µg/ml in Krebs buffer. In contrast to the detection surface, the control surface displayed a ~ 10 nm red shift on incubation with the insulin solution (section II) and returned to baseline level following the washing step with Krebs buffer (section III). This indicates that the measured response on the detection surface was due to successful capture of the insulin within the pores. It should also be noted that this surface outperformed the Ab-modified pSi both in sensitivity (19 nm EOT shift compared to 16 nm EOT shift and also detection time, 12 min compared to 60 min); highlighting the potential performance benefits from using aptamers over antibodies as bioreceptors in biosensor devices.

3.3.3 Limit of detection analysis

In order to determine the limit of detection (LOD) for each sensing interface, a calibration curve was established for each using insulin concentrations of 5 µg/ml, 10 µg/ml, 20 µg/ml, 30 µg/ml, 40 µg/ml and 50 µg/ml in Krebs buffer. Sensorgrams following the same experimental conditions at each concentration were performed, with the final ΔEOT determined for each.

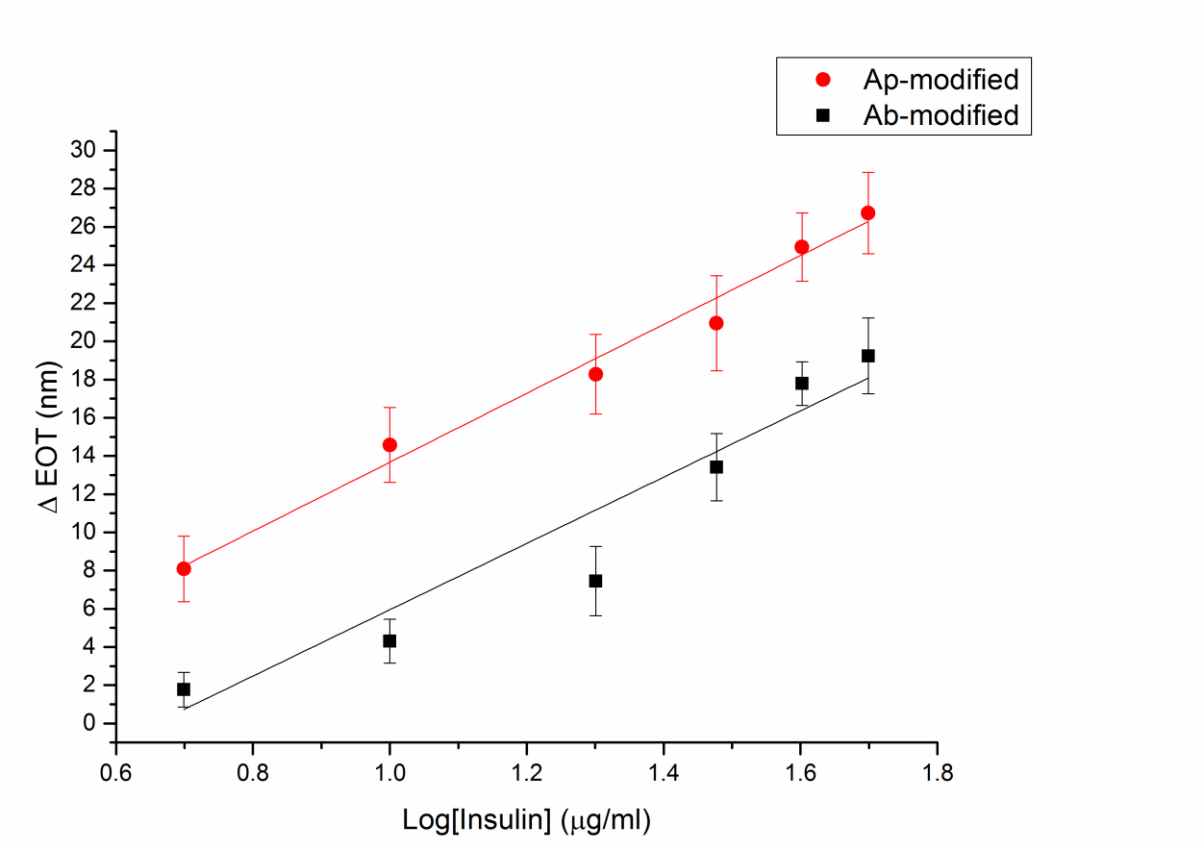

Figure 5: ΔEOT shifts obtained on Ab- and Ap- modified pSi surfaces at insulin concentrations of 5 µg/ml, 10 µg/ml, 20 µg/ml, 30 µg/ml, 40 µg/ml, 50 µg/ml in Krebs buffer. The error was calculated from the standard deviation of three individual biosensor experiments.

Figure 5 shows the ΔEOT response plotted as a function of log [Insulin] (µg/ml). The ΔEOT value increased linearly with the log of insulin concentration, regardless of the bioreceptor attached to the pSi surface. However, the ΔEOT response obtained for every insulin concentration was higher on the Ap-modified surface compared to the response on the Ab-modified surface. Moreover, the calculated R^2 value for both graphs, indicate better correlation for the Ap-modified (R^2=0.99) surface compared to the Ab-modified surface (R^2 = 0.92). The limit of detection (LOD) was calculated by applying the following equation; LOD

= 3Sa/b, where Sa is the standard deviation of the y-axis and b is the slope value. The theoretically calculated LOD on the Ab-modified surface was 4.3 µg/ml, and was 1.9 µg/ml on the Ap-modified surface. The determined LODs, maximum signal and response time all confirm a greater sensing performance on the Ap-modified surface in comparison to the Ab-modified surface. Note the the detection range we obtained is sufficient to apply the prepared biosensors to assess the quality of islets before transplantation such as islets degranulation, a common problem with islets in which islets burst insulin either due to stress, death of or dying beta cell (Bottino et al. 2004; Dai et al. ; Papas et al. 2009; Qureshi et al. 2015).

3.4 Application of Ap-modified pSi sensor to glucose-stimulated insulin secretion

In the context of determining the insulin production efficiency of islets, it is important that the demonstrated biosensor platform can detect insulin in a real sample. Often, biosensors can perform under ideal conditions in the laboratory, but fail to perform when challenged with a real sample. This is often due to the presence of complex biological components such as proteins and cell debris. In this case, an aliquot of supernatant from glucose-stimulated human islets (harvested from a donor), was used to demonstrate the biosensor's ability to measure insulin from a complex solution.

The previously presented result for spiked insulin detection in Krebs buffer demonstrated that the Ap-modified surface outperformed the Ab-modified surface. Therefore, the Ap-modified surface was applied to detect insulin secreted by human donor islets. 40,000 IEQ human islets were stimulated with 20 mM glucose for 2 h in Krebs buffer, after which the cells were centrifuged and the insulin containing supernatant was collected.

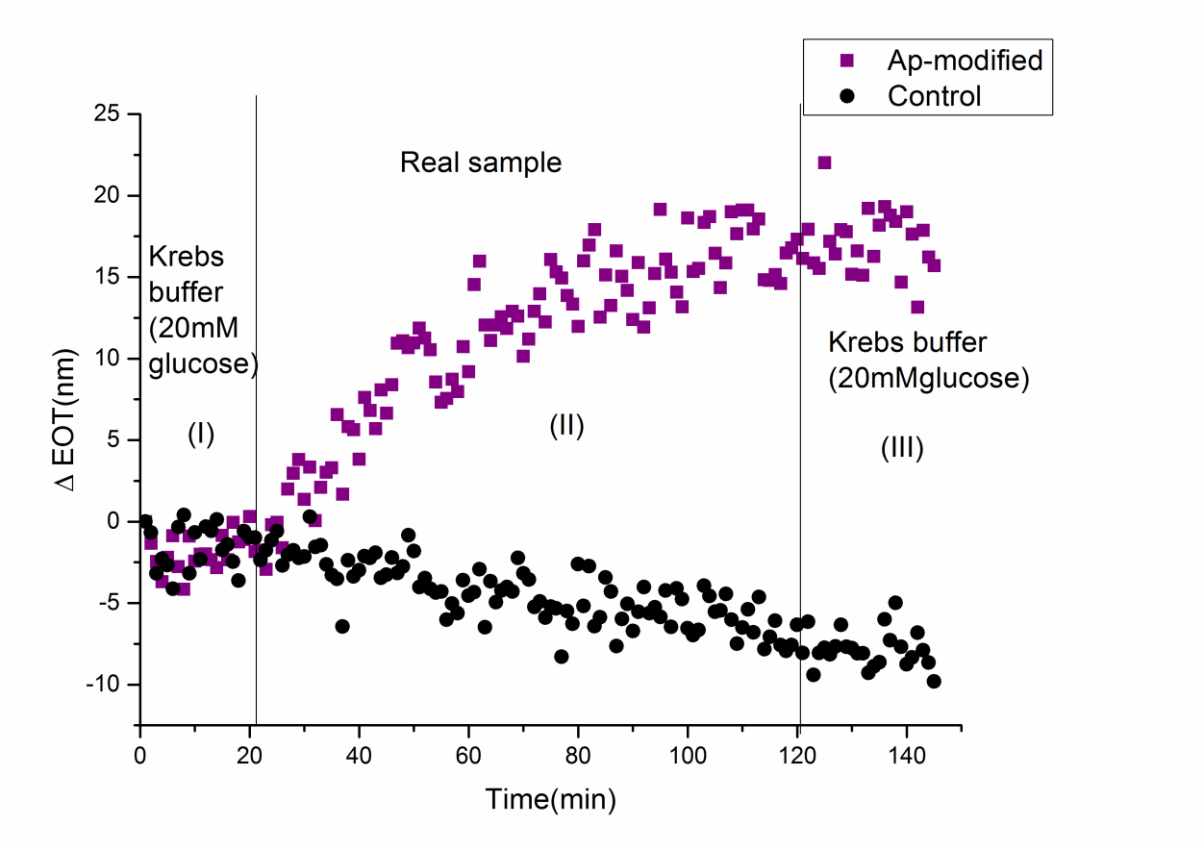

Figure 6: Sensorgram for the detection of insulin secreted by human islets upon stimulation with 20 mM glucose for 2 h in Krebs buffer using IRS.

The supernatant was then applied for a sensing experiment following the previously detailed protocol. As shown in Figure 6, there was no change to ΔEOT for the first 20 min (section I) where the surface was exposed to Krebs buffer with 20 mM glucose. The surface was then exposed to the insulin containing supernatant (section II), and a gradual increase in ΔEOT was observed during first 80 min. The ΔEOT reached equilibrium after this time and a maximum ΔEOT shift of ~ 17 nm was determined. During the washing step (section III), there was no significant change in ΔEOT and an overall red shift of ~ 17 nm was taken as the sensor reading. Applying this shift to the calibration curve obtained for the Ap-modified surface, gave an insulin concentration of 15.4 µg/ml. In addition, no significant changes to

ΔEOT were observed on the control surface, except for a small blue shift as a result of slight degradation of pSi in the aqueous medium (Alhmoud et al. 2015; Krismastuti et al. 2013). Using an ELISA, the insulin in the real sample was determined to be 16.9 +/- 0.2 µg/ml (Figure S5), in reasonable agreement with our biosensor.

4. Conclusion

Two label-free pSi based interferometric biosensing platforms were prepared using both an antibody and aptamer as the bioreceptor. This is simple platform has allowed the successful detection of insulin on both biosensing performs using IRS. It was observed that the Ap-modified surface outperformed the Ab-modified surface in terms of response value, response time and LOD. Finally, we have demonstrated the capability for the Ap-modified surface to detect insulin secreted by human islets from a donor, upon stimulation with glucose. Indeed, this is the first time a pSi based IRS sensing platform has been applied for the detection of insulin from a human islets sample.

These platforms have opened up avenues towards direct, real time detection of insulin secreted by human islets in the near future, which could be an effective method for assessing the quality of donor islets before transplantation.

Acknowledgment

The authors would like to acknowledge financial support from the Australian Research Council (ARC) Centre of Excellence in Convergent Bio-Nano Science and Technology. We would also like to thank Dr. Darling M. Rojas-Canales and Daniella Penko for assistance with islets experiments, Stuart McClure for performing SEM images and Dr Xavier Ceto Alseda with data analysis.

References

Alberti, K.G.M.M., Zimmet, P.f., 1998. Diabetic medicine 15(7), 539-553.
Alhmoud, H., Delalat, B., Elnathan, R., Cifuentes-Rius, A., Chaix, A., Rogers, M.L., Durand, J.O., Voelcker, N.H., 2015. Advanced Functional Materials 25(7), 1137-1145.
Atkinson, M.A., Eisenbarth, G.S., Michels, A.W., The Lancet 383(9911), 69-82.
Basu, S., Kanungo, J., 2011. Nanocrystalline porous silicon. INTECH Open Access Publisher.
Bottino, R., Balamurugan, A.N., Tse, H., Thirunavukkarasu, C., Ge, X., Profozich, J., Milton, M., Ziegenfuss, A., Trucco, M., Piganelli, J.D., 2004. Diabetes 53(10), 2559-2568.
Bottino, R., Trucco, M., 2015. Pediatric diabetes 16(6), 393-401.
Cha, T.-G., Baker, B.A., Sauffer, M.D., Salgado, J., Jaroch, D., Rickus, J.L., Porterfield, D.M., Choi, J.H., 2011. ACS nano 5(5), 4236-4244.
Chiang, J.L., Kirkman, M.S., Laffel, L.M., Peters, A.L., 2014. Diabetes Care 37(7), 2034-2054.
Choi, H.W., Sakata, Y., Kurihara, Y., Ooya, T., Takeuchi, T., 2012. Anal. Chim. Acta 728, 64-68.
Coffer, J.L., Whitehead, M.A., Nagesha, D.K., Mukherjee, P., Akkaraju, G., Totolici, M., Saffie, R.S., Canham, L.T., 2005. Physica status solidi (a) 202(8), 1451-1455.
Cryer, P.E., 2011. The American journal of medicine 124(11), 993-996.
Dai, C., Kayton, N.S., Shostak, A., Poffenberger, G., Cyphert, H.A., Aramandla, R., Thompson, C., Papagiannis, I.G., Emfinger, C., Shiota, M., Stafford, J.M., Greiner, D.L., Herrera, P.L., Shultz, L.D., Stein, R., Powers, A.C., The Journal of Clinical Investigation 126(5), 1857-1870.
Dancil, K.-P.S., Greiner, D.P., Sailor, M.J., 1999. J. Am. Chem. Soc. 121(34), 7925-7930.
Daniels, J.S., Pourmand, N., 2007. Electroanalysis 19(12), 1239-1257.
De la Mora, M., Lugo, J., Faubert, J., Ocampo, M., Doti, R., 2013. Porous Silicon Biosensors. INTECH Open Access Publisher.
De Stefano, L., Rea, I., Caliò, A., Politi, J., Terracciano, M., Korotcenkov, G., 2015. Porous Silicon: From Formation to Application: Biomedical and Sensor Applications, Volume Two: Biomedical and Sensor Applications, 69.
Dhanekar, S., Jain, S., 2013. Biosensors Bioelectron. 41, 54-64.
Farino, Z.J., Morgenstern, T.J., Vallaghe, J., Gregor, N., Donthamsetti, P., Harris, P.E., Pierre, N., Freyberg, R., Charrier-Savournin, F., Javitch, J.A., 2016. PloS one 11(2), e0148684.
Feltbower, R.G., Bodansky, H.J., Patterson, C.C., Parslow, R.C., Stephenson, C.R., Reynolds, C., McKinney, P.A., 2008. Diabetes care 31(5), 922-926.
Flavel, B.S., Sweetman, M.J., Shearer, C.J., Shapter, J.G., Voelcker, N.H., 2011. ACS Applied Materials & Interfaces 3(7), 2463-2471.
Grant, A., Christie, M., Ashcroft, S., 1980. Diabetologia 19(2), 114-117.
Holthausen, D., Vasani, R.B., McInnes, S.J., Ellis, A.V., Voelcker, N.H., 2012. ACS Macro Letters 1(7), 919-921.
Huh, C., Kim, B.K., Kim, W.J., Hong, J.C., Sung, G.Y., 2011. Label-free biosensor. Google Patents.
Inzucchi, S.E., Sherwin, R.S., 2011. Cecil Medicine. 24th ed. Philadelphia, Pa: Saunders Elsevier.

Jamois, C., Li, C., Gerelli, E., Orobtchouk, R., Benyattou, T., Belarouci, A., Chevolot, Y., Monnier, V., Souteyrand, E., 2011. New concepts of integrated photonic biosensors based on porous silicon.
Jane, A., Dronov, R., Hodges, A., Voelcker, N.H., 2009. Trends Biotechnol. 27(4), 230-239.
Janshoff, A., Dancil, K.-P.S., Steinem, C., Greiner, D.P., Lin, V.S.-Y., Gurtner, C., Motesharei, K., Sailor, M.J., Ghadiri, M.R., 1998. J. Am. Chem. Soc. 120(46), 12108-12116.
Kekow, J., Ulrichs, K., Müller-Ruchholtz, W., Gross, W.L., 1988. Diabetes 37(3), 321-326.
Kin, T., Senior, P., O'Gorman, D., Richer, B., Salam, A., Shapiro, A.M.J., 2008. Transplant Int. 21(11), 1029-1035.
Krismastuti, F.S., Brooks, W.L., Sweetman, M.J., Sumerlin, B.S., Voelcker, N.H., 2014a. Journal of Materials Chemistry B 2(25), 3972-3983.
Krismastuti, F.S., Pace, S., Melville, E., Cowin, A., Dargaville, T.R., Voelcker, N.H., 2013. Aust. J. Chem. 66(11), 1428-1434.
Krismastuti, F.S., Pace, S., Voelcker, N.H., 2014b. Advanced functional materials 24(23), 3639-3650.
Krismastuti, F.S.H., Cavallaro, A., Prieto-Simon, B., Voelcker, N.H., 2016. Advanced Science.
Lei, C., Xu, C., Noonan, O., Meka, A.K., Zhang, L., Nouwens, A., Yu, C., 2015. Chem. Comm. 51(71), 13642-13645.
Leitão, C.B., Cure, P., Tharavanij, T., Baidal, D.A., Alejandro, R., 2008. Current diabetes reports 8(4), 324-331.
Lérondel, G., 2015. Porous Silicon: From Formation to Application: Formation and Properties, Volume One: Formation and Properties, 217.
Lin, V.S.-Y., Motesharei, K., Dancil, K.-P.S., Sailor, M.J., Ghadiri, M.R., 1997. Science 278(5339), 840-843.
Livingstone, S.J., Levin, D., Looker, H.C., et al., 2015. JAMA 313(1), 37-44.
Low, S.P., Voelcker, N.H., Canham, L.T., Williams, K.A., 2009. Biomaterials 30(15), 2873-2880.
Luo, X., Xu, M., Freeman, C., James, T., Davis, J.J., 2013. Analytical chemistry 85(8), 4129-4134.
Mairal, T., Özalp, V.C., Sánchez, P.L., Mir, M., Katakis, I., O'Sullivan, C.K., 2008. Anal. Bioanal. Chem. 390(4), 989-1007.
Mariuzza, R., Phillips, S., Poljak, R., 1987. Annual review of biophysics and biophysical chemistry 16(1), 139-159.
McInnes, S.J.P., Turner, C.T., Al-Bataineh, S.A., Airaghi Leccardi, M.J.I., Irani, Y., Williams, K.A., Cowin, A.J., Voelcker, N.H., 2015. Journal of Materials Chemistry B 3(20), 4123-4133.
Merkl, S., Vornicescu, D., Dassinger, N., Kehrel, M., Harpel, S., Keusgen, M., 2012. physica status solidi (a) 209(5), 864-870.
Monošík, R., Streďanský, M., Šturdík, E., 2012. Acta Chimica Slovaca 5(1), 109-120.
Montane, J., 2015. Enliven: Surg Transplant 1(1), 007.
Mora, M.B.d.l., Ocampo, M., Doti, R., Lugo, J.E., Faubert, J., 2013. Porous Silicon Biosensors.
Nathan, D.M., 2014. Diabetes Care 37(1), 9-16.
Ohkubo, T., 1994. Biomed. Chromatogr. 8(6), 301-305.
Pacholski, C., Sartor, M., Sailor, M.J., Cunin, F., Miskelly, G.M., 2005. J. Am. Chem. Soc. 127(33), 11636-11645.
Papas, K.K., Suszynski, T.M., Colton, C.K., 2009. Current opinion in organ transplantation 14(6), 674.
Paty, B.W., 2005. Paediatrics & Child Health 10(1), 38-40.

Perumal, V., Hashim, U., 2014. Journal of Applied Biomedicine 12(1), 1-15.
Pi, J., Bai, Y., Zhang, Q., Wong, V., Floering, L.M., Daniel, K., Reece, J.M., Deeney, J.T., Andersen, M.E., Corkey, B.E., 2007. Diabetes 56(7), 1783-1791.
Piper, M., Seidenfeld, J., Aronson, N., 2004.
Qu, F., Yang, M., Lu, Y., Shen, G., Yu, R., 2006. Anal. Bioanal. Chem. 386(2), 228-234.
Qureshi, F.M., Dejene, E.A., Corbin, K.L., Nunemaker, C.S., 2015. Cell Calcium 57(5–6), 366-375.
Rafiee, B., Fakhari, A.R., 2013. Biosensors Bioelectron. 46, 130-135.
Raftery, L.J., Grewal, Y.S., Howard, C.B., Jones, M.L., Shiddiky, M.J., Carrascosa, L.G., Thurecht, K.J., Mahler, S.M., Trau, M., 2016. Chem. Comm. 52(33), 5730-5733.
Reta, N., Michelmore, A., Saint, C., Prieto-Simón, B., Voelcker, N.H., 2016. Biosensors Bioelectron.
Rickels, M.R., Schutta, M.H., Mueller, R., Markmann, J.F., Barker, C.F., Naji, A., Teff, K.L., 2005. Diabetes 54(11), 3205.
Rother, K.I., Harlan, D.M., The Journal of Clinical Investigation 114(7), 877-883.
Rother, K.I., Harlan, D.M., 2004. The Journal of clinical investigation 114(7), 877-883.
Sang, S., Zhang, W., Zhao, Y., 2013. Review on the Design Art of Biosensors. INTECH Open Access Publisher.
Schumacher, S., Seitz, H., 2016. New biotechnology.
Sciacca, B., Secret, E., Pace, S., Gonzalez, P., Geobaldo, F., Quignard, F., Cunin, F., 2011. Journal of Materials Chemistry 21(7), 2294-2302.
Shabir, Q., 2014. Biodegradability of Porous Silicon. Handbook of Porous Silicon, pp. 395-401. Springer.
Shang, Y., Zhao, W., Xu, E., Tong, C., Wu, J., 2010. Biosensors Bioelectron. 25(5), 1056-1063.
Sharma, S., Johnson, R.W., Desai, T.A., 2004. Biosensors Bioelectron. 20(2), 227-239.
Singh, V., Krishnan, S., 2015. Analytical chemistry 87(5), 2648-2654.
Skrivarhaug, T., Bangstad, H.-J., Stene, L., Sandvik, L., Hanssen, K., Joner, G., 2006. Diabetologia 49(2), 298-305.
Song, S., Wang, L., Li, J., Fan, C., Zhao, J., 2008. TrAC Trends in Analytical Chemistry 27(2), 108-117.
Steiner, P., Lang, W., 1995. Thin Solid Films 255(1), 52-58.
Steward, M.W., Lew, A.M., 1985. J. Immunol. Methods 78(2), 173-190.
Strehlitz, B., Nikolaus, N., Stoltenburg, R., 2008. Sensors 8(7), 4296-4307.
Sweetman, M.J., Harding, F.J., Graney, S.D., Voelcker, N.H., 2011a. Applied Surface Science 257(15), 6768-6774.
Sweetman, M.J., Ronci, M., Ghaemi, S.R., Craig, J.E., Voelcker, N.H., 2012. Advanced Functional Materials 22(6), 1158-1166.
Sweetman, M.J., Shearer, C.J., Shapter, J.G., Voelcker, N.H., 2011b. Langmuir 27(15), 9497-9503.
Szili, E.J., Jane, A., Low, S.P., Sweetman, M., Macardle, P., Kumar, S., Smart, R.S.C., Voelcker, N.H., 2011. Sensors Actuators B: Chem. 160(1), 341-348.
The National Institute of Diabetes and Digestive and Kidney Diseases US, U.S. DEPARTMENT OF HEALTH AND HUMAN SERVICES.
Tombelli, S., Minunni, M., Mascini, M., 2007. Biomol. Eng. 24(2), 191-200.
Tong, W.Y., Sweetman, M.J., Marzouk, E.R., Fraser, C., Kuchel, T., Voelcker, N.H., 2016. Biomaterials 74, 217-230.
Touahir, L., Allongue, P., Aureau, D., Boukherroub, R., Chazalviel, J.-N., Galopin, E., Gouget-Laemmel, A., de Villeneuve, C.H., Moraillon, A., Niedziółka-Jönsson, J., 2010. Bioelectrochemistry 80(1), 17-25.

Trabucchi, A., Iacono, R.F., Guerra, L.L., Faccinetti, N.I., Krochik, A.G., Arriazu, M.C., Poskus, E., Valdez, S.N., 2014. PLOS ONE 8(12), e84099.
Van Der Windt, D.J., Bottino, R., Casu, A., Campanile, N., Cooper, D.K., 2007. Xenotransplantation 14(4), 288-297.
Verdian-Doghaei, A., Housaindokht, M.R., Bozorgmehr, M.R., Abnous, K., 2015. J. Biomol. Struct. Dyn. 33(6), 1153-1163.
Vo-Dinh, T., 2014. Biomedical Photonics Handbook: Biomedical Diagnostics. CRC press.
Vo-Dinh, T., Cullum, B., 2000. Fresenius J. Anal. Chem. 366(6-7), 540-551.
Voelcker, N.H., Alfonso, I., Ghadiri, M.R., 2008. ChemBioChem 9(11), 1776-1786.
Wang, J., Musameh, M., 2004. Anal. Chim. Acta 511(1), 33-36.
Wang, J., Tangkuaram, T., Loyprasert, S., Vazquez-Alvarez, T., Veerasai, W., Kanatharana, P., Thavarungkul, P., 2007. Anal. Chim. Acta 581(1), 1-6.
Wang, P.-Y., Clements, L.R., Thissen, H., Hung, S.-C., Cheng, N.-C., Tsai, W.-B., Voelcker, N.H., 2012. RSC Advances 2(33), 12857-12865.
Yagati, A.K., Park, J., Cho, S., 2016. Sensors 16(1), 109.
Yoshida, W., Mochizuki, E., Takase, M., Hasegawa, H., Morita, Y., Yamazaki, H., Sode, K., Ikebukuro, K., 2009. Biosensors Bioelectron. 24(5), 1116-1120.
Yu, Q., Zhang, Y., Wang, H., Brash, J., Chen, H., 2011. Acta Biomater. 7(4), 1550-1557.
Yu, Y., Guo, M., Yuan, M., Liu, W., Hu, J., 2016. Biosensors Bioelectron. 77, 215-219.
Zhou, W., Huang, P.-J.J., Ding, J., Liu, J., 2014. Analyst 139(11), 2627-2640.

Highlights

- Porous silicon based optical biosensor using Interferometric reflectance spectroscopy (IRS) used for insulin detection in islet cell culture
- Surface characterisation using scanning electron microscopy (SEM), Fourier transform infrared (FTIR) spectroscopy performed
- Aptamer and antibody used and compared as bioreceptors
- Application of aptamer modified surface for detection of insulin secreted by human islet on stimulation with glucose
-